Development of an Omnidirectional Neck for Evaluation of Sports, Automobiles and Automotive Protective Equipment

G. Fonseca and P.A. Cripton
Orthopaedic and Injury Biomechanics Group, Departments of Mechanical Engineering and Orthopaedics and the School of Biomedical Engineering, University of British Columbia, Vancouver, BC Canada

ABSTRACT

Objective

The kinematic responses of a cervical sub-axial functional spinal unit (FSU) will be reproduced by modelling vertebrae after healthy males of 30-45 years of age, modelling intervertebral discs (IVD) and ligaments to replicate impacts of a sleeping individual and ensuring the surrogate can withstand repeatable injurious impacts (ie. is durable).

Methods

Cervical vertebrae were 3D-printed and CNC milled in order to be used in the construction of FSU surrogates (FSU-1, comprised of C3-C5 and FSU-2, comprised of C3-C4) and dimensional accuracy of the vertebral design and fabrication processes were assessed. Once the assessment was complete, ligaments and discs were attached and adhered, respectively, to the vertebrae in order to create FSUs. The surrogates were tested in axial rotation and flexion-extension, and the kinematic results were captured and compared to cadaver data from published studies.

Results

The maximum percent error of vertebrae dimensions was 14.29% and the greatest error was 1.52 mm which is small enough to suggest human error in measurement. The kinematic results of FSU-1 in axial rotation exhibited a sigmoidal curve that was in line with cadaver data, however, it took only 0.1 Nm for the surrogate to reach 10° of rotation and thus it was much less stiff than the published cadaver data. FSU-2 kinematic trends also had a sigmoidal shape in axial rotation and in flexion-extension, although the range of motion in axial rotation, neutral zone in flexion-extension (range in which the spine rotates with minimal or no applied torque) and maximum degrees of extension at specified torques were still outside of the cadaveric range. The neutral zone in axial rotation and range of motion in flexion were in line with published cadaveric data which is promising.

Conclusions

The results are trending in the right direction and with further FSU component refinement, reproducing the kinematic responses of sub-axial functional spinal units is achievable and will aid in the construction of a surrogate biofidelic omnidirectional neck. The ultimate goal is to use the surrogate neck to improve safety equipment meant to protect the head and neck in transportation, occupational and sports settings.

INTRODUCTION

An estimated 500 000 people worldwide suffer a spinal cord injury (SCI) annually (WHO, 2013). The most common SCI is to the cervical spine (Singh, 2014), and more specifically, to the C4-C5 level (DeVivo, 2002). An injury at this level would result in tetraplegia, which, at a minimum, is the partial loss of sensation and control in all four limbs and the torso. Tetraplegia drastically decreases quality of life with suicide rates increasing fivefold within eleven years (DeVivo, 1991). Incidence of traumatic brain injuries (TBI) is even more staggering, with approximately 69 million occurring annually (Dewan, 2019). Even a mild TBI, such as a concussion, can cause health problems like headaches, fatigue, inability to focus, depression and traumatic stress for up to a year (Losoi, 2016). In addition to the physical toll, patients must carry a substantial economic burden. The lifetime expenses can be anywhere from $80,000.00 US, when accounting for inflation, for a mild TBI (McGregor, 1997), up to $3,030,000.00 US for an SCI resulting in complete tetraplegia (full loss of senses and control below the injury level) (Lenehan, 2012).

SCIs and TBIs are most likely to occur in males between the ages of 15-30 (Singh, 2014) and 15-24 (Nguyen, 2016; CDC, 2016) respectively. Frequently resulting in several decades of disability and/or paralysis for the injured person. The top three scenarios in which both injury types occur are vehicle collisions, fall- and sport-related impacts (Cripps, 2011 and Singh, 2014). Safety devices meant to protect against SCIs and TBIs, such as helmets, air bags, compliant floors and seat belts, in the aforementioned scenarios are often evaluated with the use of an anthropometric test device (ATD). The Hybrid III neck is the most commonly used ATD neck, as it is specified in automotive and helmet standards, and consists of a one-piece aluminum-elastomer mold surrounding a steel cable to provide stability (Foster, 1977). It is only biofidelic (matches human kinematic biomechanics with high fidelity) in high speed rear or frontal vehicle collisions (Foster, 1977; Nightingale, 1991; Gwin, 2010; Fréchède, 2009). Unfortunately, the Hybrid III is used in impact scenarios in which it is not biofidelic, such as helmet and rollover testing (Viano, 2006; Moffatt, 2003). Other ATDs include the THOR, BioRid II and The Nelson and Cripton Neck (Nelson and Cripton, 2010), but similar to the Hybrid III, they are not biofidelic for all injury scenarios and they do not closely represent the anatomy of a human neck. The overall natural curvature of the cervical spine provides stability and the individual vertebral geometry defines the range of motion (Kapandji, 1974) Currently, there is no single surrogate appropriate for the multiplane loading that often occurs in real-world scenarios (Nelson and Cripton, 2010).

Our long-term project objective is to create a biofidelic, omnidirectional, (i.e. having biofidelic responses in all directions) surrogate cervical spine (vertebrae C1-C7) that can represent three preparedness levels; asleep, awake and not braced, and awake and braced. The surrogate neck would be able to mimic responses of both males and females at all ages. This research, however, is a first step towards the overall objective. It aims to produce a biofidelic, cervical, sub-axial functional spinal unit (FSU; two or more vertebrae and the intervertebral discs between them) with passive muscle properties, simulating a sleeping individual, that can withstand repeatable injurious impacts (ie. durable). This will be done by modelling vertebrae after CT scans of healthy adult males at 30-45 years of age and modelling intervertebral discs and ligaments to replicate impacts of a sleeping individual (ie. passive muscle activity).

METHODS

Ideal Vertebrae Construction

The first step of this research was to obtain computer-generated 3D models of C3-C5 (Figure 1 left) from an anatomical drawing and modify them to include ligament anchor points and mounting holes (Figure 1 right). This was accomplished using SolidWorks (SolidWorks 64-bit, Student Engineering Kit 2017, Dassault Systems, Velizy-Villacoublay, France). The vertebrae constructed this way were symmetrical and without deformities. These ideal, modified vertebrae were 3D-printed and an FSU (FSU-1) was constructed by attaching silicone ligaments and adhering checkered rubber sheets, in place of intervertebral discs, with Gorilla Glue (Gorilla Glue Inc.). It was secured superiorly and inferiorly to mounting brackets (Figure 2).

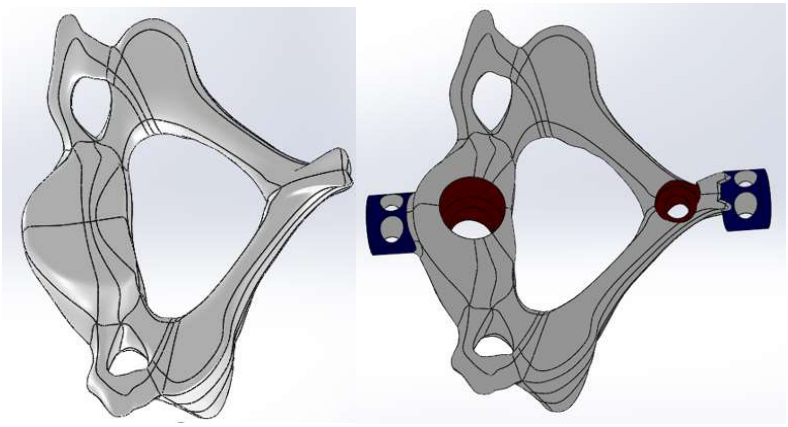

Figure 1: Ideal vertebra (left) and ideal vertebrae with custom attachment points (right).

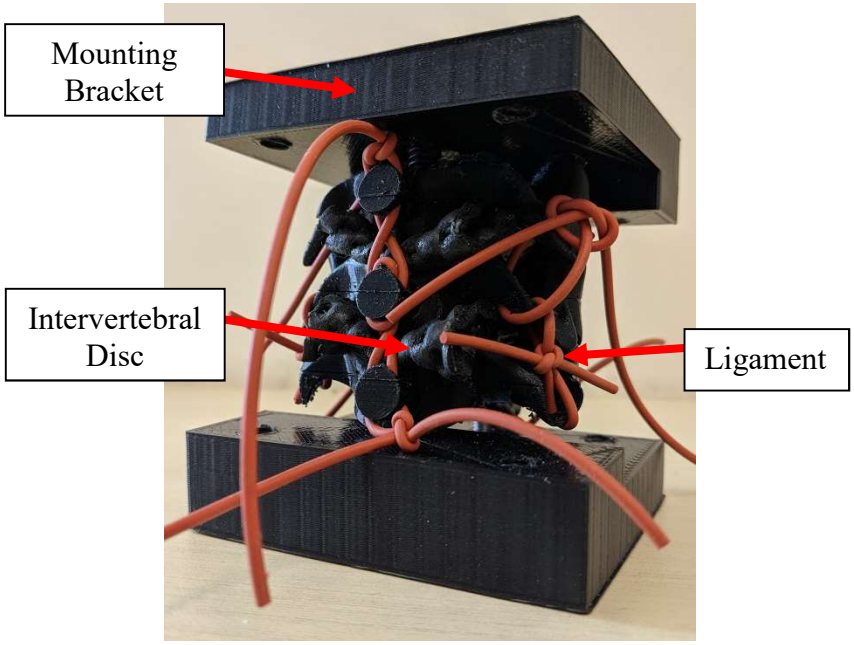

Figure 2: FSU-1 (Ideal, modified C3-C5 secured to mounting brackets with silicone cord used as ligaments and checkered rubber sheets used as intervertebral discs).

The next step was to build an ideal, modified FSU using a CNC milled C3 and a 3D-printed C4 (FSU-2) (Figure 3). FSU-2 components were updated to include Gorilla Tough Braid (Berkley) ligaments, crimped with metal ferrules, and 3M VHB 4991 double sided tape (The 3M Company) as intervertebral discs, removing the need for additional adhesive. The intervertebral disc was constructed with anatomically correct dimensions (Gilad, 1984), based on caliper readings.

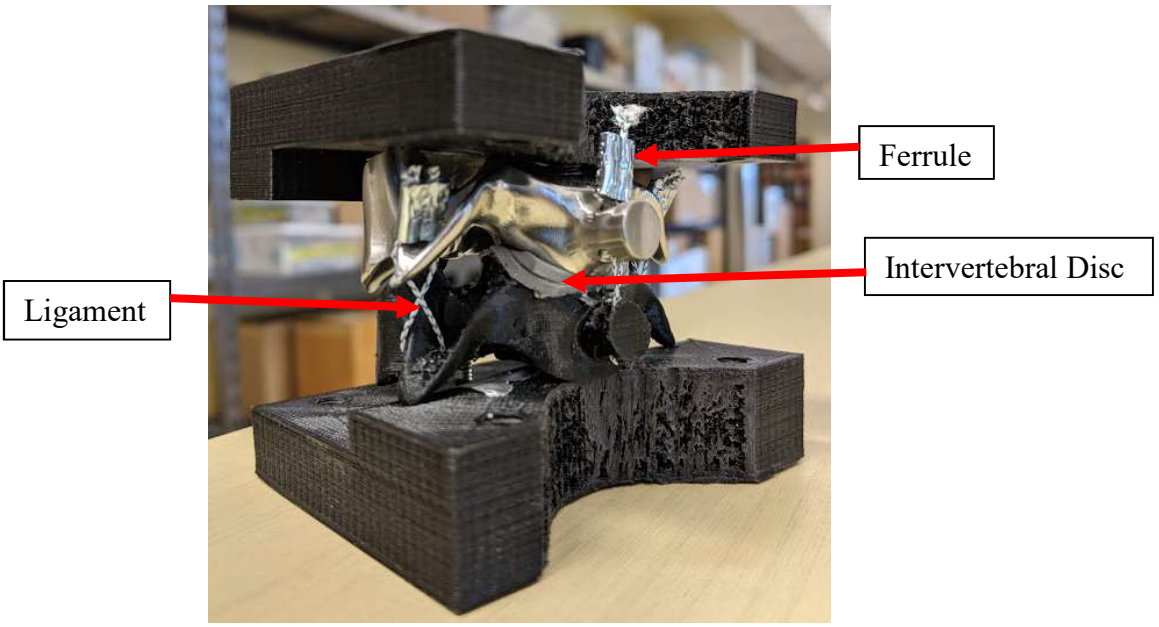

Figure 3: FSU-2 (Ideal, modified CNC milled 316 SST C3 and ideal, modified 3D-printed C4, secured to mounting brackets. Complete with Gorilla Tough Braid ligaments, crimped with metal ferrules, and 3M VHB 4991 double sided tape as intervertebral discs).

Pure moment testing

FSU-1 underwent axial rotation in our custom spine machine (Figure 4). The spine machine is able to apply a pure torque to the centre of the FSU through the use of a motor and counter balance. It can be oriented to test FSUs in axial rotation, lateral bending and flexion-extension.

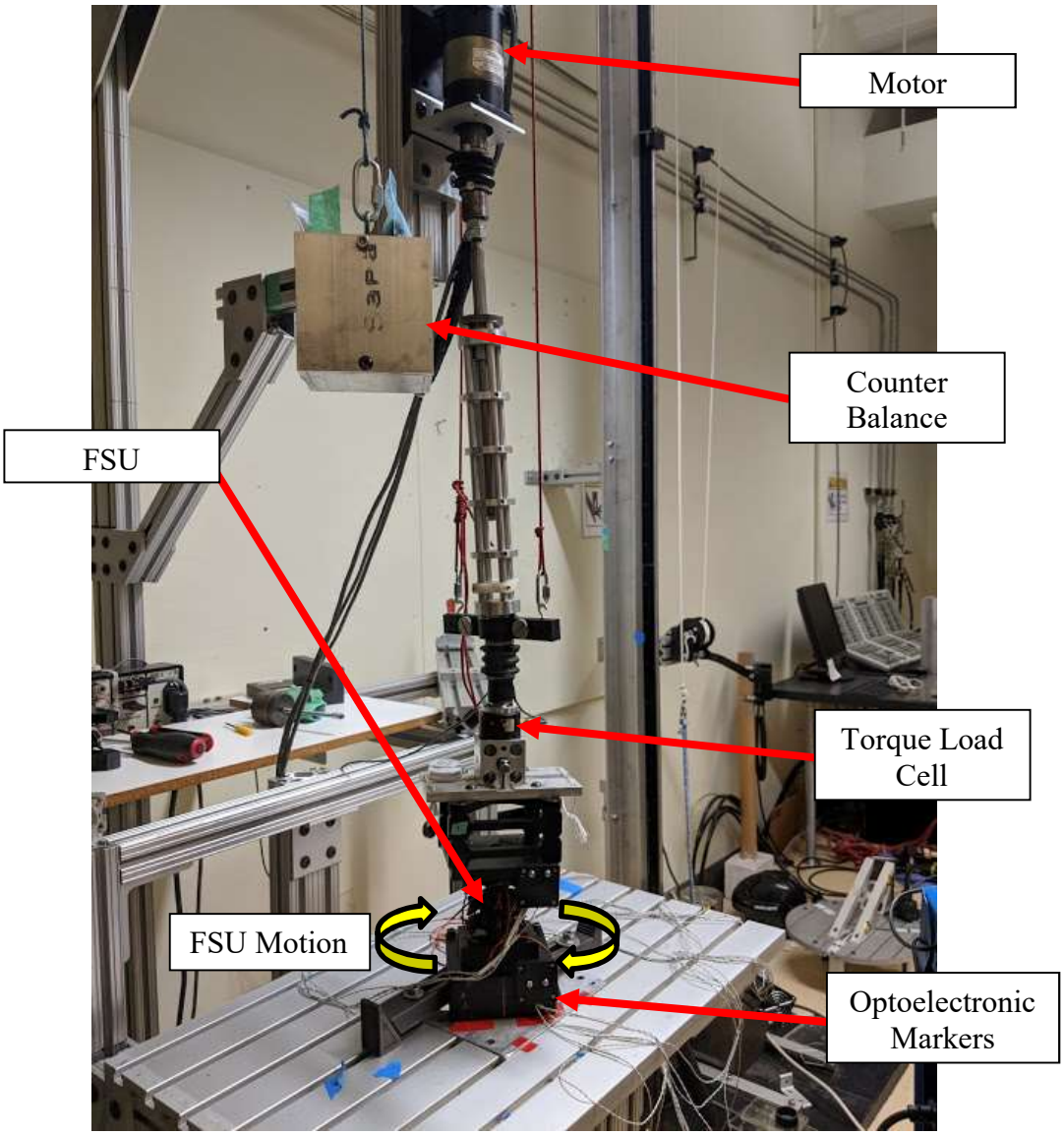

Figure 4: Axial rotation in custom spine machine.

Once velocity was set to 2 deg/s and the target torque requirement was set to 0.1 Nm, the spine machine began to rotate at constant velocity until it hit its target torque, then began to rotate in the other direction until again hitting its target torque, a total of three times. The kinematic results were captured with a torque load cell and an optoelectronic motion analysis system, Optotrak (Northern Digital Inc.). The degrees of rotation versus force results were compared to previous cadaver tests in our lab to assess biofidelity. The original plan was to test FSU-1 in all three motions, however, the C5 vertebra fractured upon completion of the axial rotation testing.

The same procedure was used to test FSU-2 in the spine machine in axial rotation, at a velocity of 1 deg/s and a target torque of 1.5 Nm. Flexion-extension tests were also performed at a velocity of 1 deg/s and a target torque of 1 Nm. Again, the plan was to test the FSU in all three motions, however, even after raising the fill density to 100% on the 3D-printed vertebra, the FSU still fractured upon completion of the axial rotation and flexion-extension testing.

CT Scan Generated Vertebrae Construction

The final vertebrae will not be ideal as in FSU-1 and FSU-2, but from CT scans of patients recruited from the Vancouver Spine Surgery Institute. This was a retrospective database review of patients who have been assessed by the Spine Service for a thoracic and/or lumbar spine injury and have had a CT scan of the entire spine at Vancouver General Hospital (VGH). Patients who have/had spinal disease including advanced degeneration, spinal deformity, structural injury, or surgery in the cervical, T1 or T2 regions were **not** eligible for admission into the study. Fellowship-trained spine surgeon Dr. Shun Yamamato used patient notes and visual cues from the CT scans to determine if the patient met the aforementioned exclusion criteria. As the selected CT scans are not yet available for review, the *CT scan to 3D object* process was tested with an anonymous C3-C4 cadaver CT scan. The CT scan used to create a realistic 3D vertebra by segmenting C3 and converting the 3D rendering to an .stl file with the use of Analyze 12 (Analyze 64-bit, v12.0, Analyze Direct Inc., Kansas, USA). The .stl file was in contrast to the previous 'ideal' and thus unrealistic models. The segmented C3 was then imported into MeshLab 2016 (MeshLab 64-bit, v2016.12, ISTI-CNR, Pisa, Italy) in order to remove artifacts. Next, the file was imported into SolidWorks and modified to include intervertebral disc and ligament attachment points and finally, the segmented, modified vertebra was 3D-printed (Figure 5) to exhibit the imperfections of a real vertebra.

Figure 5: Segmented, modified C3 (from CT-Scan images).

Vertebra Construction Accuracy Assessment

In order to assess accuracy, CT scan dimensions were taken (Figure 6), identical to Wu's measurements (Wu, 2015) using a DICOM image viewer InVesalius 3 (InVesalius 64-bit v3.1.1, CTI Renato Archer, Campinas, Sao Paulo, Brazil) and compared to dimensions of the segmented, modified 3D .stl file, measured with SolidWorks, to assess accuracy.

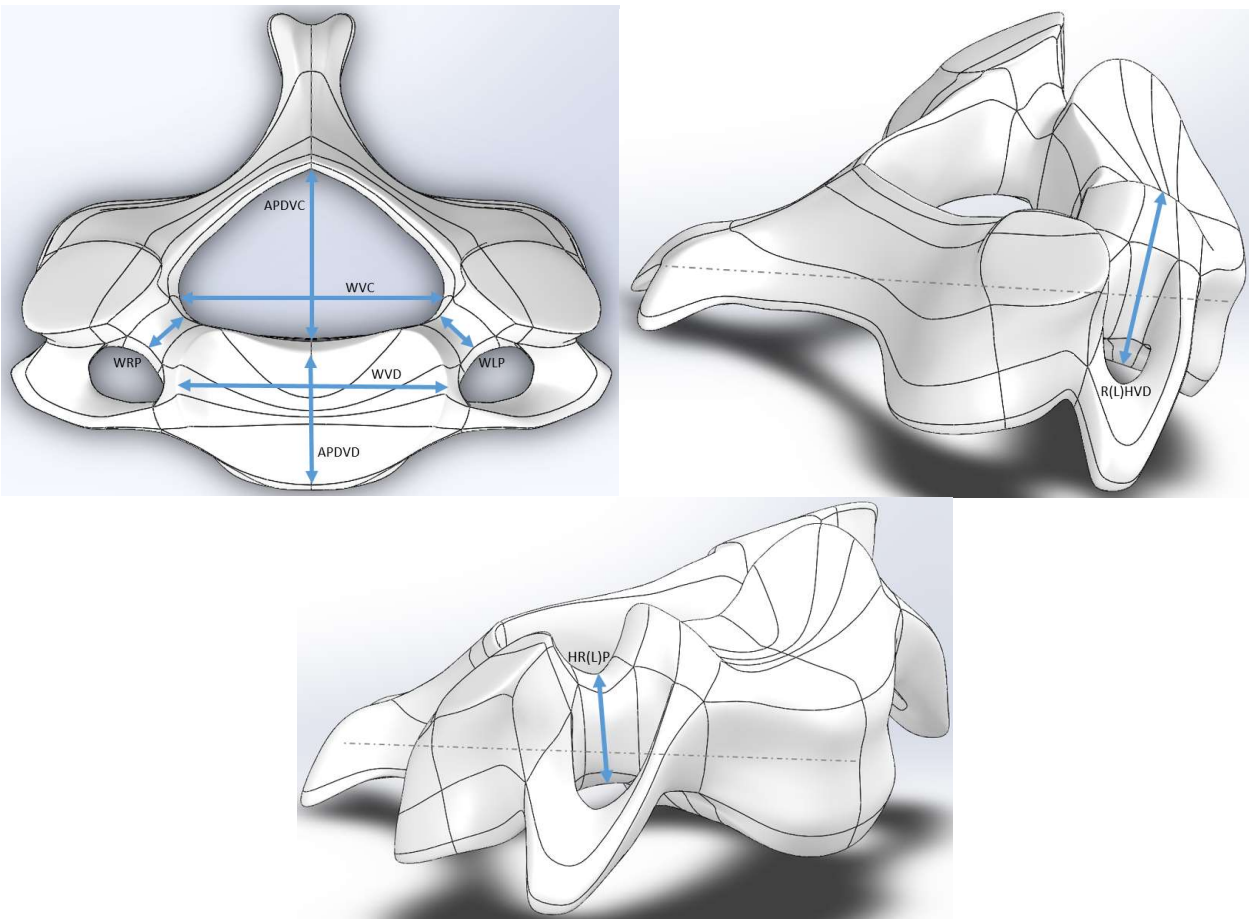

Figure 6: Vertebral dimensions measured.

Durability was increased by CNC milling the ideal, modified C3 using 316 Stainless Steel (Figure 7). Again, dimensions were taken using the Optotrak motion analysis system to digitize points on the surface (0.1 mm system accuracy) and results were compared to the computer-generated model, obtained using SolidWorks as previously described, to assess dimensional accuracy.


Figure 7: Ideal, modified C3, CNC milled using 316 Stainless Steel

RESULTS

The axial rotation versus torque results from the surrogate FSU-1 had a sigmoidal curve. The custom spine machine allowed rotation in the surrogate to reach approximately 10 degrees of rotation at 0.1 Nm with a speed of 2 deg/s (Figure 8).

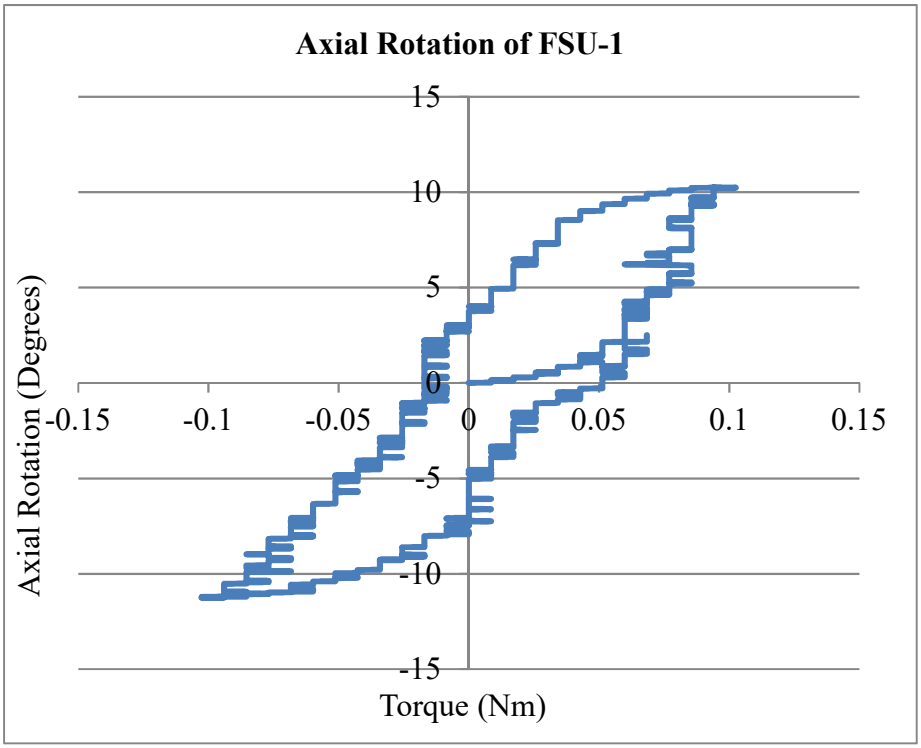

Figure 8: Sigmoidal axial rotation curve of FSU-1.

The ideal, modified CNC milled vertebra had a maximum percent error of 9.26% across all measured dimensions and the highest error was 1.52 mm (Table 1). The segmented part had a maximum percent error of 14.29% and the highest error was 1.52 mm (Table 2).

Table 1: Dimensional Accuracy of CNC Milling Process

Ideal C3	SolidWorks Measurement (mm)	CNC Milled Measurement (mm)	Percent Error	Error (mm)
Width of vertebral body (WVB)	26.92	25.91	3.77%	1.02
Anteroposterior diameter of vertebral body (APDVB)	13.21	12.95	1.92%	0.25
Left height of vertebral body (LHVB)	13.72	14.99	9.26%	1.27
Right height of vertebral body (RHVB)	13.72	14.99	9.26%	1.27
Width of vertebral canal (WVB)	31.50	29.97	4.84%	1.52
Anteroposterior diameter of vertebral canal (APDVC)	20.32	20.07	1.25%	0.25
Width of right pedicle (WRP)	6.10	6.60	8.33%	0.51
Height of right pedicle (HRP)	5.59	6.10	9.09%	0.51
Width of left pedicle (WLP)	6.10	6.60	8.33%	0.51
Height of left pedicle (HLP)	5.59	6.10	9.09%	0.51

Table 2: Dimensional Accuracy of CT Scan to 3D Computer Generated File Process

CT Scan C4	InVesalius Measurement (mm)	SolidWorks Measurement (mm)	Percent Error	Error (in)
Width of vertebral body	22.86	22.10	3.33%	0.76
Anteroposterior diameter of vertebral body	14.73	15.75	6.90%	1.02
Left height of vertebral body	16.00	14.48	9.52%	1.52
Right height of vertebral body	15.24	14.99	1.67%	0.25
Width of vertebral canal	24.64	24.13	2.06%	0.51
Anteroposterior diameter of vertebral canal	12.95	13.46	3.92%	0.51
Width of right pedicle	7.11	6.35	10.71%	0.76
Height of right pedicle	6.60	6.86	3.85%	0.25
Width of left pedicle	5.33	6.10	14.29%	0.76
Height of left pedicle	7.87	7.62	3.23%	0.25

FSU-2 rotated 14 degrees at 1.5 Nm in the custom spine machine. The neutral zone (range in which the spine rotates with minimal (0.2 Nm) or no applied torque) is roughly 24 degrees (Figure 9). The general trend exhibits a more obvious sigmoidal shape when compared to the results of FSU-1.

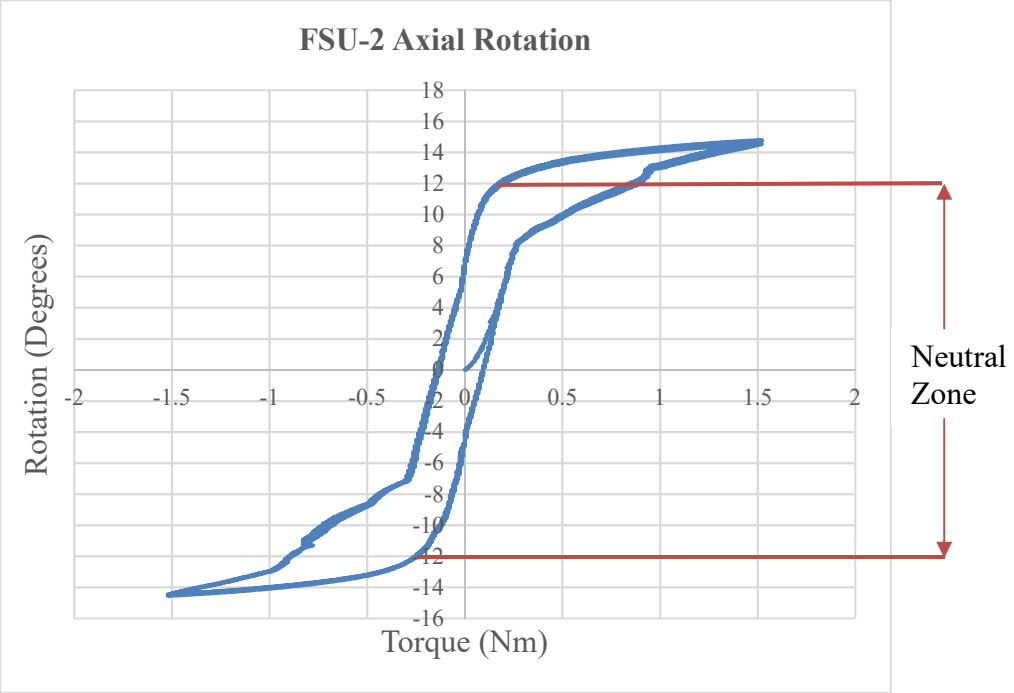

Figure 9: Axial rotation in the custom spine machine of FSU-2.

FSU-2 extended 6 degrees and flexed 8 degrees at 1 deg/s and 1 Nm in the custom spine machine. The neutral zone is approximately 7.5 degrees. The general trend is sigmoidal the range of motion was higher in flexion than extension.

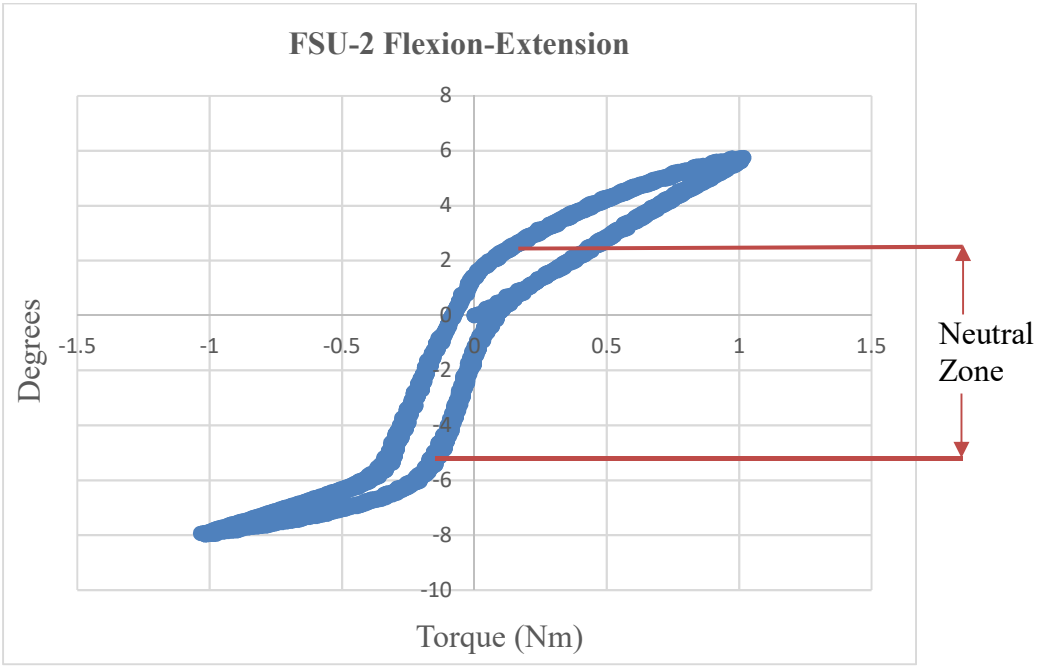

Figure 10: Flexion-Extension in the custom spine machine of ideal, modified FSU, including CNC milled C3 and 3D-printed C4.

DISCUSSION

Kinematics

FSU-1 was meant to provide a basic understanding of the complex behavior inherent to FSUs. C3-C5 was selected as a starting point as our lab has cadaveric lateral bending, axial rotation and flexion-extension data from osteoligamentous C3-C5 FSUs. Unfortunately, as previously mentioned, FSU-1 fractured due to the axial rotation testing. The axial rotation results were still valid therefore we began by analyzing the curve shape. The sigmoidal curve is apparent in both FSU-1 and cadaveric data (Yoganadan, 2008) which gives an indication that the vertebral anatomy does in fact have an impact on the range of motion. We then began to look into the kinematics and noted that our lab's previous cadaver C3-C5 FSU rotated 10 degrees between 0.1 and 1 Nm of torque (Unpublished Melnyk, 2017) as opposed to FSU-1 that reached 10 degrees of rotation at 0.1 Nm consistently. After watching FSU-1 through its range of motion and comparing results, it became obvious that stiffer ligaments and/or a disc material/adhesive that increases friction is/are required.

As there are many moving parts in an FSU (vertebrae, discs and ligaments), it was decided that moving forward, the focus would shift to a two vertebrae model. After using stiffer ligament material and a disc material with more surface area to hopefully increase friction, the overall axial rotation trend exhibited a more exaggerated sigmoidal curve than FSU-1, and was more in line with cadaveric results. It was also able to withstand more torque as it rotated 14 degrees at 1 Nm. While this was not in the range of published data, as Yoganandan 2008 showed between 4.25 and 7.5 degrees of axial rotation for cadavers between ages 23 and 44 (Yoganandan, 2008), it was a step in the right direction. Yoganandan's trends also show a netural zone of 5-9 degrees, therefore, based on a 0.2 Nm neutral zone distinction, FSU-2's 7.5 degree neutral zone is in the biofidelic range. In flexion-extension, Wheeldon 2006 showed that at 1 Nm of torque, C3-C4 FSU was capable of 3 to 4 degrees of extension, 4-10 degrees of flexion and a neutral zone of 3.5 degrees (Wheeldon, 2006). While FSU-2 was able to extend by two more degrees, and the neutral zone was larger by 4.5 degrees, its flexion of 8 degrees was in line with literature. The greater range of motion in flexion than extension was also in line with literature.

After testing FSU-1 and FSU-2, it became increasingly clear that component level testing will be required for a more efficient design process. Compression tests will be carried out on potential disc material and the material with highest biofidelity, when compared to Cripton's work (Cripton, 1999), will be selected. Similarly, tension tests will be carried out on potential ligament material and the materials with the highest biofidelity, when compared to Mattucci's work (Mattucci, 2011), will be selected.

Finally, it is worth noting that although most SCI and TBIs do not occur at ages 30-45, there is not enough cadaver data to support an FSU modeled after the most common age of injury (15-30) which is why the subsequent fifteen-year age range was selected. Additionally, the ideal CT scan would be that of a 50^{th} percentile individual, however, of the CT scans to be obtained from VGH, none were 50^{th} percentile. Despite not being in the 50^{th} percentile, the FSU constructed from CT scans will still provide anatomically correct vertebrae, as opposed to existing ATD designs.

Dimensional Accuracy

Although the highest percent error is 14.29%, the highest dimensional error, when comparing the CT scan to the segmented, modified .stl file and the ideal, modified .stl file to the ideal, modified CNC milled part, is 1.52 mm. An error of this magnitude is small enough to suggest user error in measurement. Note that dimensions were taken from the segmented, modified .stl file on Solidworks as opposed to the 3D printed segmented, modified vertebra because accuracy of the segmentation process was required, not of the 3D printing process. Once the segmented, modified vertebra is CNC milled, measurements will be taken on the physical part as opposed to the .stl file.

CONCLUSIONS

Reproducing the kinematic responses of sub-axial FSUs will aid in the construction of a biofidelic omnidirectional durable surrogate neck. The process of constructing a C4-C5 FSU will inform future construction of a C3-C7 FSU. Future research will see progression on a C1-C2 FSU that will be attached the rest of the surrogate cervical spine in order to achieve the overall research objective. The final goal is to use the full surrogate neck to evaluate, improve and optimize head and neck safety equipment for transportation, occupational and sports settings.

ACKNOWLEDGEMENTS

I would like to thank Dr. Brian Kwon, Leilani Reichl and Shun Yamammoto for their support in CT scan retrieval as well as ICORD and OIBG for the use of their facilities.

REFERENCES

Spinal Cord Injury. (2013). WHO. Retrieved from http://www.who.int/mediacentre/factsheets/fs384/en/

Singh, A., Tetreaulty, L., Kalsi-Ryan, S., Nouri, A., Fehlings, M.G. (2014). Global Prevalence and Incidence of Traumatic Spinal Cord Injury. Journal of Clinical Epidemiology, Journal Vol. 6, 309–331.

DeVivo, M.J. (2002). Epidemiology of traumatic spinal cord injury. Journal of Spinal Cord Medicine, Journal Vol. 24, 69–81.

DeVivo, M.J., Black, K.J., Richards, J.S., Stover, S.L. (1991). Suicide Following Spinal Cord Injury. Paraplegia, Journal Vol. 29, 620-627.

Dewan, M.C., Rattani, A., Gupta, S., Baticulon, R.E., Hung, Y.C., Punchak, M., Agrawal, A., Adelye, A.O., Shirme, M.G., Rubiano, A.M., Rosenfeld, J.V., Park, K.B., (2019). Estimating the global incidence of traumatic brain injury. Journal of Neurosurgery, Paper Journal Vol. 130(4), 1039-1408.

Losoi, H., Silverberg, N.D., Wäljas, M., Turunen, S., Rosti-Ostajävari, E., Helminen, M., Luoto, T.M., Julkunen, J., Öhman, J., Iverson, G.L. (2016). Recovery from Mild Traumatic Brain Injury in Previously Healthy Adults. Journal of Neurotrauma, Journal Vol. 33(8), 766-776.

Mcgregor, K. Pentland, B. (1997). Head injury rehabilitation in the U.K.: an economic perspective. Social Science and Medicine, Journal Vol. 45(2), 295-303.

Lenehan, B., Street, J., Kwon, B.K., Noonan, V., Zhang, H., Fisher, C.G., Dvorak, M.F. (2012). The epidemiology of traumatic spinal cord injury in British Columbia, Canada. Spine Philadelphia, PA (1976), Journal Vol. 37(4)-321-329.

Nguyen, R., Fiest, K.M., McChesney, J., Kwon, C.S., Jette, N., Frolkis, A.D., Atta, C., Mah, S., Dhaliwal, H., Reid, A., Pringsheim, T., Dykeman, J., Gallagher, C. (2016). The International Incidence of Traumatic Brain Injury: A Systematic Review and Meta-Analysis. Canadian Journal of Neurological Sciences, Journal Vol. 43(6), 774-785.

Rates of TBI-related Emergency Department Visits by Age Group — United States, 2001–2010. (2016). CDC. Retrieved from https://www.cdc.gov/traumaticbraininjury/data/rates_ed_byage.html

Cripps, R.A., Lee, B.B., Wing, P., Weerts, E., Mackay, J., Brown, D. (2011). A Global Map for Traumatic Spinal Cord Injury Epidemiology: Towards a Living Data Repository for Injury Prevention. Spinal Cord, Journal Vol. 49(4), 493–501.

Foster J.K., Kortge, J.O., Wolanin, M.J. (1977). Hybrid III-A Biomechanically Based Crash Test Dummy. Proc. of the 21st Stapp Car Crash Conference, SAE Paper No. 770938, 3268-3283.

Nightingale R.W., (1991). The Influence of End Condition on Human Cervical Spine Injury Mechanisms. Proc. 35th Stapp Car Crash Conf, Society of Automotive Engineers, Paper No. 912915, 391-399.

Gwin J.T., Chu, J.J., Diamond, S.G., Halstead, P.D., Crisco, J.J., Greenwald, R.M. (2009). An Investigation of the NOSCAE Linear Impactor Test Method Based on In Vivo Measures of the Head Impact Acceleration in the American Football. Journal of Biomechanical Engineering, Journal Vol. 132(1), 011006–011009.

Fréchède, B., McIntosh, I., Grzebieta, R., Bambach, M. (2009). Hybrid III ATD in Inverted Impacts: Influence of Angle on Neck Injury Risk Assessment. Annals of Biomedical Engineering, Journal Vol. 37(7), 1403–1414.

Viano, D.C., Pellman, E.J., Withnall, C., Shewchenko, N. (2006) Concussion in professional football: performance of newer helmets in reconstructed game impacts--Part 13. Neurosurgery, Journal Vol. 59(3), 591-606.

Moffatt, E., Hare, B., Hughes, R., Lewis, L., Iiyama, H., Curzon, A., Cooper, E. (2003). Head Excursion of Restrained Human Volunteers and Hybrid III Dummies in Steady State Rollover Tests Annual Proceedings, Association for the Advancement of Automotive Medicine, Journal Vol. 47, 445-465.

Nelson T.S., Cripton, P.A. (2010). A New Biofidelic Sagittal Plane Surrogate Neck for Head-First Impacts. Traffic Injury Prevention, Journal Vol. 11(3):309–319.

Kapandji, I.A., (1974). The Physiology of the Joints: Volume Three: The Trunk and the Vertebral Column. 2nd edn. Churchill Livingstone, London, UK.

Wu, A.M., Shao, Z.X., Wang, J.S., Yang, X.D., Weng, W.Q., Wang, X.Y., Xu, H.Z., Chi, Y.L., Lin, Z.K. (2015). The Accuracy of a Method for Printing Three-Dimensional Spinal Models. PLOS One, Journal Vol. 10(4), e0124291.

Gilad, I., Nissan, M. (1986). A Study of Vertebrae and Disc Geometric Relations of the Human Cervical and Lumbar Spine. Spine Philadelphia, PA (1976), Journal Vol. 11(2), 154-157.

Yoganandan, N., Stemper, B.D., Pintar, F.A., Baisden, J.L., Shender, B.S., Paskoff, G. (2008). Normative Segment-Specific Axial and Coronal Angulation Corridors of Subaxial Cervical Column in Axial Rotation. Spine Philadelphia, PA (1976), Journal Vol. 33(5), 490-496.

Melnyk, A. (2017). Unpublished. Orthpaedic Injury Biomechanics Group.

Wheeldon, J.A., Pintar, F.A., Knowles, S., Yoganandan, N. (2006). Experimental flexion extension data corridors for validation of finite element models of the young, normal cervical spine. Journal of Biomechanics, Journal Vol. 39(2), 375-380.

Cripton, P.A. (1999). Load-Sharing in the Human Cervical Spine. PhD Thesis, Queen's University, Kingston, Canada.

Mattucci, S. (2011). Strain Rate Dependent Properties of Younger Human Cervical Spine Ligaments. MASc Thesis, University of Waterloo, Waterloo, Canada.